

# Covalent DNA Adducts Formed in Mouse Epidermis from Dibenz[*a,j*]anthracene: Evidence for the Formation of Polar Adducts

Wanda Baer-Dubowska,<sup>†</sup> Raghunathan V. Nair,<sup>†</sup> Cecilia Cortez,<sup>‡</sup>  
Ronald G. Harvey,<sup>‡</sup> and John DiGiovanni<sup>\*,†</sup>

The University of Texas M. D. Anderson Cancer Center, Science Park-Research Division,  
P.O. Box 389, Smithville, Texas 78957, and The Ben May Institute, University of Chicago,  
Chicago, Illinois 60637

Received September 19, 1994<sup>®</sup>

The formation of deoxyribonucleoside adducts in mouse epidermis has been examined following topical application of [<sup>3</sup>H]dibenz[*a,j*]anthracene (DB[*a,j*]A) or by <sup>32</sup>P-postlabeling following topical application of unlabeled DB[*a,j*]A, DB[*a,j*]A *trans*-3,4-diol or the *anti*- or *syn*-3,4-diol 1,2-epoxides. A single topical application of [<sup>3</sup>H]DB[*a,j*]A at a dose of 400 nmol per mouse led to the formation of 11 detectable covalent DNA adducts. Seven of these DNA adducts were tentatively identified based on cochromatography with marker adducts using high-pressure liquid chromatography (HPLC). The presence of both deoxyguanosine (dGuo) as well as deoxyadenosine (dAdo) adducts formed from bay-region *anti*- and *syn*-3,4-diol 1,2-epoxides of DB[*a,j*]A was revealed. The major bay-region diol epoxide DNA adduct formed in mouse epidermis following topical application of [<sup>3</sup>H]DB[*a,j*]A was tentatively identified as the (4*R*,3*S*)-diol (2*S*,1*R*)-epoxide bound through *trans* addition of the exocyclic amino group of dGuo, although substantial amounts of the corresponding dAdo adduct were also detected. In addition, a K-region 5,6-oxide-dAdo adduct was tentatively identified in HPLC chromatograms based on cochromatography with an authentic marker adduct. <sup>32</sup>P-Postlabeling analysis of DB[*a,j*]A-DNA adducts formed in mouse epidermis after topical application of unlabeled compound confirmed the presence of bay-region diol epoxide DNA adducts similar to those observed after application of [<sup>3</sup>H]DB[*a,j*]A. However, <sup>32</sup>P-postlabeling analysis also revealed the presence of more polar covalent DNA adducts in epidermal DNA samples from DB[*a,j*]A-treated mice. These more polar DNA adducts represented a significant proportion of the <sup>32</sup>P-labeled material recovered in HPLC chromatograms. While the exact nature of these adducts remains unknown at present, they had retention times identical to polar DNA adducts formed following topical application of DB[*a,j*]A *trans*-3,4-diol and may represent bis-dihydrodiol epoxide DNA adducts. The present results indicate that a rather broad spectrum of DNA adducts arises following topical application of DB[*a,j*]A to mouse epidermis.

## Introduction

The metabolic activation of polycyclic aromatic hydrocarbons (PAH)<sup>1</sup> to reactive electrophilic intermediates and their subsequent covalent binding to epidermal DNA are believed to be critical events in the initiation stage of mouse skin tumorigenesis. For most PAH, the ultimate carcinogenic metabolites are vicinal diol epoxides, most frequently of the "bay region" type (1-3). Dibenz[*a,j*]anthracene (DB[*a,j*]A), one of the three possible isomeric dibenzanthracenes (DBA), has not been extensively studied in terms of its metabolism and metabolic activation compared to the other isomers; however, its

mutagenic and carcinogenic activity has been demonstrated (4-6). According to the bay-region theory (7), 3,4-diol 1,2-epoxides metabolically generated from DB[*a,j*]A via the *trans*-3,4-dihydrodiol should be ultimate carcinogenic metabolites. Studies performed in our laboratory demonstrated that (±)*anti*-DB[*a,j*]A diol epoxide [(±)*anti*-DB[*a,j*]ADE] was significantly more active than the parent compound as a skin tumor-initiator, suggesting that the metabolic formation of this diol epoxide and its covalent modification of DNA may, in fact, be involved in the process of tumor initiation by DB[*a,j*]A (6).

Structural characterization of the DNA adducts derived from the reaction of (±)*anti*-DB[*a,j*]ADE and pure enantiomers of both the *syn*- and *anti*-diol epoxide of DB[*a,j*]A with calf thymus DNA showed that these compounds bound extensively to both deoxyguanosine (dGuo) and deoxyadenosine (dAdo) residues (8-10). Examination of the covalent DNA adducts formed in cultured mouse keratinocytes exposed to [<sup>3</sup>H]DB[*a,j*]A revealed formation of a variety of bay-region diol epoxide DNA adducts including both dGuo and dAdo adducts (10). There is considerable evidence emerging to indicate that binding to dAdo might be critical for the tumor-initiating activity of some PAH. Adducts with dAdo have been

\* To whom correspondence should be addressed.

<sup>†</sup> The University of Texas M. D. Anderson Cancer Center.

<sup>‡</sup> The Ben May Institute.

<sup>®</sup> Abstract published in *Advance ACS Abstracts*, February 1, 1995.

<sup>1</sup> Abbreviations: PAH, polycyclic aromatic hydrocarbons; B[a]P, benzo[*a*]pyrene; DMBA, 7,12-dimethylbenz[*a*]anthracene; DBA, dibenzanthracene; DB[*a,j*]A, dibenz[*a,j*]anthracene; (±)*anti*-DB[*a,j*]ADE, (±)-*trans*-3,4-dihydroxy-*anti*-1,2-epoxy-1,2,3,4-tetrahydrodibenz[*a,j*]anthracene; *syn*-DB[*a,j*]ADE, (±)-*trans*-3,4-dihydroxy-*syn*-1,2-epoxy-1,2,3,4-tetrahydrodibenz[*a,j*]anthracene; dGuo, deoxyguanosine; dAdo, deoxyadenosine; dCyt, deoxycytidine; 7-MeBA, 7-methylbenz[*a*]anthracene; PNK, polynucleotide kinase; PEI, poly(ethyleneimine); MO, molecular orbital; DB[*a,h*]A, dibenz[*a,h*]anthracene; FA, fluoranthene.

identified in DNA from animal tissues or cultured cells treated with a number of hydrocarbons (11–14) and in some cases represent major covalent DNA adducts (e.g., 7,12-dimethylbenz[*a*]anthracene). Recent studies of the DNA binding of the highly mutagenic *syn*-diol epoxide derivatives of benz[*c*]phenanthrene and benzo[*g*]chrysene show preferential formation of dAdo adducts, which accounts for 80–90% of the total adducts (15–17). In our recent studies examining the nature of *c*-Ha-*ras* mutations in skin papillomas initiated by DB[*a,j*]A, we found exclusively A<sup>182</sup> → T transversion mutations (18). These data implicated dAdo adducts in the tumor-initiating activity of DB[*a,j*]A.

In the present study, we examined the major DB[*a,j*]A-DNA adducts formed in mouse epidermis after topical application of DB[*a,j*]A and several of its metabolic derivatives using two different approaches: (i) analysis of <sup>3</sup>H-labeled metabolites covalently bound to DNA and (ii) a <sup>32</sup>P-postlabeling technique (19). In our previous studies using mouse keratinocytes in culture, only a small proportion (≤15%) of the radioactivity associated with the isolated DNA represented the above-mentioned covalent adducts (10). Furthermore, a significant proportion of this DNA-associated radioactivity eluted with the solvent front in HPLC chromatograms. We now report that both K-region oxide and bay-region diol epoxide DNA adducts as well as more polar DNA adducts are detectably present in mouse skin treated with DB[*a,j*]A. The current findings help provide an explanation for our previous results (10) as well as demonstrate that a major proportion of the DNA damage produced by DB[*a,j*]A in mouse epidermis *in vivo* results from the formation of relatively polar metabolites. The results are discussed in terms of DNA adduct studies with other DBA isomers as well as the relationship to DB[*a,j*]A-induced mutations in murine *c*-Ha-*ras*.

## Materials and Methods

**Chemicals.** Caution: DB[*a,j*]A and the derivatives of DB[*a,j*]A described within this paper have been determined to be carcinogenic to laboratory animals. Hence, protective clothing and appropriate safety procedures should be followed when working with these compounds.

DB[*a,j*]A was provided by the NCI Chemical Carcinogen Reference Standard Repository, a function of the Division of Cancer Cause and Prevention, National Cancer Institute, NIH, Bethesda, MD, or synthesized as previously described (20). (±)-*anti*-DB[*a,j*]ADE was also prepared as previously described (21). The K-region (±)DB[*a,j*]A 5,6-oxide was also prepared from the parent hydrocarbon by the general method previously described (22). Thus, reaction of DB[*a,j*]A (1.1 g, 3.94 mmol) with osmium tetroxide (1.0 g, 3.94 mmol) in 50 mL of pyridine was carried out for 3 h at room temperature by method B described for the preparation of the 4,5-*cis*-dihydrodiol of benzo[*a*]pyrene (22). The crude DB[*a,j*]A *cis*-dihydrodiol (1.1 g) was acetylated with acetic anhydride-pyridine, purified by chromatography on a column of Florisil, and recrystallized from benzene-hexane (1:1). A solution of the *cis*-diacetate with sodium methoxide (120 mg) in 20 mL of methanolic tetrahydrofuran (1:1) was stirred at 60 °C for 30 min, worked up by partition between ether and water, dried over MgSO<sub>4</sub>, and evaporated to dryness to yield pure DB[*a,j*]A 5,6-*cis*-dihydrodiol (860 mg, 70% overall), mp 216–218 °C (dec), NMR (300 MHz, Me<sub>2</sub>SO-*d*<sub>6</sub> + D<sub>2</sub>O) δ 9.22 (s, 1, H<sub>14</sub>), 9.09 (d, 1, H<sub>13</sub>), 8.35 (d, 1, H<sub>1</sub>), 8.09 (s, 1, H<sub>7</sub>), 7.39–7.99 (m, 8, aryl), 4.84 (d, 1, H<sub>6</sub>), 4.72 (d, 1, H<sub>5</sub>); in the absence of D<sub>2</sub>O, hydroxyl proton peaks were detected as doublets at δ 5.39 and 4.18. Anal. Calcd for C<sub>22</sub>H<sub>16</sub>O<sub>2</sub>: C, 84.59; H, 5.16. Found: C, 84.45; H, 5.07. Oxidation of the *cis*-dihydrodiol (500 mg, 1.6 mmol) with 2,3-dichloro-5,6-dicyano-1,4-benzoquinone (900 mg,

10 mmol) in 20 mL of tetrahydrofuran for 1 h at room temperature furnished a brick red precipitate of the quinone. The reaction was quenched by the addition of water, and the precipitate was filtered, washed with water, and dried to yield DB[*a,j*]A 5,6-dione essentially quantitatively (480 mg). Anal. Calcd for C<sub>22</sub>H<sub>12</sub>O<sub>2</sub>: C, 85.70; H, 3.92. Found: C, 85.55; H, 4.08. Reduction of the quinone (308 mg, 1 mmol) with excess NaBH<sub>4</sub> (1.2 g) in 300 mL of ethanol with O<sub>2</sub> bubbling through the solution was carried out for 3 days; the course of reaction was followed by HPLC analysis. Conventional workup gave the crude 5,6-*trans*-dihydrodiol (1.1 g). Pure DB[*a,j*]A 5,6-*trans*-dihydrodiol was obtained by acetylation with acetic anhydride-pyridine followed by chromatography on Florisil and deacetylation with NaOCH<sub>3</sub> in methanolic tetrahydrofuran (1:1) using the procedure employed for the DB[*a,j*]A 5,6-*cis*-dihydrodiol; (172 mg, 55% overall), mp > 240 °C (dec), NMR (500 MHz, Me<sub>2</sub>SO-*d*<sub>6</sub>) δ 9.14 (s, 1, H<sub>14</sub>), 9.02 (d, 1, H<sub>13</sub>, J<sub>12,13</sub> = 8.3 Hz), 8.26 (d, 1, H<sub>1</sub>, J<sub>1,2</sub> = 7.6 Hz), 8.11 (s, 1, H<sub>7</sub>), 7.36–7.95 (m, 8, aryl), 4.64 (d, 1, H<sub>6</sub>, J<sub>5,6</sub> = 9.4 Hz), 4.54 (d, 1, H<sub>5</sub>, J<sub>5,6</sub> = 9.4 Hz); in the absence of D<sub>2</sub>O, hydroxyl proton peaks were detected as doublets at δ 5.66 and 5.76. Anal. Calcd for C<sub>22</sub>H<sub>16</sub>O<sub>2</sub>: C, 84.59; H, 5.16. Found: C, 84.64; H, 5.04. Treatment of the *trans*-dihydrodiol (78 mg, 0.25 mmol) with the dimethyl acetal of dimethylformamide (119 mg, 2 mmol) in a refluxing solution of dimethylformamide (3 mL) and tetrahydrofuran (9 mL) for 3 days (reaction was monitored by HPLC) furnished DB[*a,j*]A 5,6-oxide (30 mg, 41%) as a white solid, mp 160–162 °C (dec), NMR (500 MHz, CDCl<sub>3</sub>) δ 9.34 (s, 1, H<sub>14</sub>), 8.74 (d, 1, H<sub>13</sub>, J<sub>12,13</sub> = 8.2 Hz), 8.37 (d, 1, H<sub>1</sub>, J<sub>1,2</sub> = 8.0 Hz), 8.07 (s, 1, H<sub>7</sub>), 7.36–7.86 (m, 8, aryl), 4.68 (d, 1, H<sub>6</sub>, J<sub>5,6</sub> = 4.4 Hz), 4.57 (d, 1, H<sub>5</sub>, J<sub>5,6</sub> = 4.0 Hz). Anal. Calcd for C<sub>22</sub>H<sub>14</sub>O: C, 89.77; H, 4.79. Found: C, 89.70; H, 4.63. The (±)*syn*-DB[*a,j*]ADE was synthesized by the method previously employed for the preparation of other related PAH *syn*-diol epoxide isomers (23).

[G-<sup>3</sup>H]DB[*a,j*]A obtained in several different lots (specific activity range 1.75–3.48 Ci/mmol) was prepared by Chemsyn Science Laboratories (Lenexa, KS) by exposure of unlabeled DB[*a,j*]A (30-mg lots) to 10 Ci of tritiated water under appropriate conditions. Labile tritium was removed, and radiochemical purity was determined by TLC on silica gel in hexane/benzene (9:1). Radiochemical purity of the final product supplied by Chemsyn Science Laboratories was ~84 ± 5% for three different lots. Alternatively, for some experiments [7-<sup>3</sup>H]DB[*a,j*]A (specific activity 22.8 Ci/mmol) was utilized. This material was prepared from 7-bromodibenz[*a,j*]anthracene by catalytic reduction as described (24). 7-Bromodibenz[*a,j*]anthracene was synthesized by the overnight reaction of the parent hydrocarbon (500 mg, 1.8 mmol) with *N*-bromosuccinimide (320 mg, 1.8 mmol) and FeCl<sub>3</sub>·6H<sub>2</sub>O (15 mg) in refluxing CCl<sub>4</sub> (200 mL). The product mixture was cooled to room temperature, then filtered through a short column of Florisil, and eluted with CH<sub>2</sub>Cl<sub>2</sub>. The fractions were recombined and chromatographed on a second Florisil column eluted with benzene-hexane to provide 7-bromodibenz[*a,j*]anthracene (630 mg, 91%) as a white solid melting at 250–253 °C after recrystallization from benzene-hexane: NMR (CDCl<sub>3</sub>) δ 9.94 (s, 1, H<sub>14</sub>), 8.90 (d, 2, H<sub>1,13</sub>, J<sub>1,2</sub> = 8.2 Hz), 8.38 (d, 2, H<sub>6,8</sub>, J<sub>5,6</sub> = 9.2 Hz), 7.87 (d, 2, H<sub>4,10</sub>, J<sub>3,4</sub> = 7.6 Hz), 7.77 (d, 2, H<sub>5,9</sub>, J<sub>5,6</sub> = 9.2 Hz), 7.72 (m, 2, H<sub>2,12</sub>), 6.63 (m, 2, H<sub>3,11</sub>). Substitution in the 7-position is confirmed by the absence of the singlet at δ 8.37 ppm characteristic of the parent hydrocarbon and the downfield shift of the signal for the H<sub>6,8</sub> protons adjacent to the site of bromine substitution. Anal. Calcd for C<sub>22</sub>H<sub>13</sub>Br: C, 73.97; H, 3.67; Br, 22.37. Found: C, 74.10; H, 3.77; Br, 22.18. Prior to use in DNA adduct studies, the specific [<sup>3</sup>H]DB[*a,j*]A used was further purified by preparative HPLC as previously described (23).

RNase A (EC 3.1.4.22) was obtained from Worthington Biochemical Co. (Freehold, NJ) while DNase I (bovine pancreas, EC 3.1.4.5), micrococcal nuclease (*Staphylococcus aureus*, EC 3.1.31.1), snake venom phosphodiesterase (*Crotalus atrox*, EC 3.1.4.1), apyrase, calf thymus DNA, and ATP were obtained from Sigma Chemical Co. (St. Louis, MO). Calf spleen phosphodiesterase (EC 3.1.16.1) and 3'-phosphatase-free T4 polynucleotide

kinase (PNK) (EC 2.7.1.78) was purchased from Boehringer Mannheim Biochemicals (Indianapolis, IN). Guanidine isothiocyanate was supplied by Bethesda Research Laboratories Inc. (Gaithersburg, MD). [<sup>3</sup>H]dAdo, [<sup>3</sup>H]dGuo, and [<sup>3</sup>H]dCyt (10–22 Ci/mmol) were obtained from ICN Laboratories (Irvine, CA), and a nick translation system was provided by Gibco BRL (Gaithersburg, MD). [ $\gamma$ -<sup>32</sup>P]ATP was supplied by DuPont, NEN (Boston, MA). Macheray-Nagel poly(ethyleneimine)–cellulose (PEI–cellulose) TLC plates were obtained from Alltech Associates, Inc. (Deerfield, IL), and a Zorbax phenyl-modified reverse-phase HPLC column was obtained from Mac-Mod Analytical, Inc. (Chadds Ford, PA).

**Preparation of Deoxyribonucleoside Hydrocarbon Adduct Markers.** The DNA adduct markers of DB[a,j]A metabolites used in the present study were prepared according to the procedure described previously (8, 10). Under similar reaction conditions, solutions of either unlabeled calf thymus DNA or calf thymus DNA radioactively labeled by a nick translation procedure with [<sup>3</sup>H]dGuo, [<sup>3</sup>H]dAdo, or [<sup>3</sup>H]dCyt in 0.01 M Tris-HCl buffer (pH 7.0) were individually reacted with the (+)- or (–)-*anti*- or ( $\pm$ )-*syn*-diol epoxides of DB[a,j]A or the K-region ( $\pm$ )-DB[a,j]A 5,6-oxide to produce the respective adduct markers.

**DNA Adduct Formation in Vivo.** Female Sencar mice (aged 7–9 weeks) obtained from the National Cancer Institute, Frederick, MD, were used for in vivo experiments. Mice were shaved on the dorsal side 2 days prior to treatment. Mice were treated by topical application to the shaved area of skin with 400 nmol of [<sup>3</sup>H]DB[a,j]A (400–800  $\mu$ Ci; 12–14 animals per group). For <sup>32</sup>P-postlabeling analysis, mice (3–4 animals per group) were treated with 1600 nmol of unlabeled DB[a,j]A or ( $\pm$ )-*trans*-DB[a,j]A 3,4-diol, and 400 nmol of unlabeled ( $\pm$ )-*anti*- or *syn*-DB[a,j]A diol epoxide. Animals were sacrificed 3 or 24 h after treatment depending on the compound. DNA was isolated from epidermis using guanidine isothiocyanate and then successive phenol and chloroform/isoamyl alcohol extraction followed by treatment with RNase as described previously (25–28).

**HPLC Analysis of <sup>3</sup>H-Labeled DB[a,j]A–DNA Adducts.** DNA samples were hydrolyzed sequentially using DNase I, snake venom phosphodiesterase, and alkaline phosphatase as described previously (25). DNA hydrolysates were subsequently applied to a short column of Sephadex LH-20 (0.9  $\times$  3 cm) and washed with water (10 mL) to remove unhydrolyzed DNA and unmodified deoxyribonucleosides. The less polar hydrocarbon–DNA adducts were then eluted with 6–10 mL of methanol. Methanol phases from six to eight experimental groups of animals (80–100 mice total) were subsequently pooled and evaporated under N<sub>2</sub> for further analysis. The methanol-soluble material was analyzed by HPLC using a Shimadzu LC6A liquid chromatograph equipped with a Beckman Ultrasphere ODS column (4.6 mm  $\times$  25 cm) and UV (254 nm) and fluorescence detectors (ex 293 nm, em 405 nm). The gradient system for separating DB[a,j]A–DNA adducts was as follows: (a) 50 min hold at 47% methanol in water; (b) 47–60% methanol in water gradient (linear, 50 min); (c) 60–100% methanol in water gradient (linear, 40 min). B[a]P-9,10 diol was used as an internal standard. The levels of individual adduct were expressed as femtomole per milligram of epidermal DNA based on the percentage of radioactivity represented by each peak and total binding levels as estimated after purification on Sephadex LH-20 columns.

**<sup>32</sup>P-Postlabeling Analysis.** DNA samples (50  $\mu$ g) were hydrolyzed to 3'-nucleotides essentially as described (29). Briefly, samples were incubated at 37 °C with micrococcal nuclease (80 mU/ $\mu$ g of DNA) in 15  $\mu$ L of 3 mM *N,N*-bis(2-hydroxyethyl)glycine (bicine, pH 9.0) and 0.5 mM CaCl<sub>2</sub>. After 2 h, 23  $\mu$ L of 20 mM sodium acetate (pH 5.0) and spleen phosphodiesterase (1.6 mU/ $\mu$ g of DNA) was added, and the samples incubated at 37 °C for another 2 h. Adducts were extracted from the resulting hydrolysate (equivalent to 30  $\mu$ g of DNA) by modification of the 1-butanol enrichment protocol (30) as follows: DNA digests (80.4  $\mu$ L) were diluted to the equivalent of 0.0375  $\mu$ g of DNA/ $\mu$ L in water containing ammonium formate (pH 3.5) and tetrabutyl-

ammonium chloride (final concentration 10 and 1 mM, respectively). DNA adducts were removed from the mixture by extracting twice with an equal volume of water-saturated 1-butanol. Residual deoxyribonucleoside 3'-monophosphates were removed from the 1-butanol by back-extracting three times with an equal volume of water. The pH of the final butanol phase was adjusted to 7.6 by the addition of 4.4  $\mu$ L of 200 mM Tris-HCl (pH 7.6). Following evaporation to dryness in a speed-vac, adduct residues were reconstituted in 15.3  $\mu$ L of water and 3.5  $\mu$ L of labeling buffer (100 mM bicine–NaOH, pH 7.6; 100 mM MgCl<sub>2</sub>; 100 mM dithiothreitol; 10 mM spermidine). Two microliters of 3'-phosphatase-free T4 PNK (10 U/ $\mu$ L) and 10  $\mu$ L of [ $\gamma$ -<sup>32</sup>P]ATP (>5000 Ci/mmol; 10 Ci/ $\mu$ L) were added, and the 5'-phosphorylation of adducted nucleotides with <sup>32</sup>P was catalyzed by incubation at 37 °C for 2.5 h. Following incubation, excess ATP was converted to orthophosphate by incubation with 150 mU of apyrase for 1 h in 37 °C.

[<sup>3</sup>H]dGuo- and [<sup>3</sup>H]dAdo-labeled calf thymus DNA reacted with ( $\pm$ )-*anti*-DB[a,j]ADE were digested and enriched for adducts using the same procedure described in the preceding paragraph. 3'-Nucleotides were again converted to 3',5'-diphosphodeoxyribonucleosides in the presence of unlabeled ATP (2 mM) and T4 PNK (40 U).

**HPLC Analysis of <sup>32</sup>P-Postlabeled DB[a,j]A–DNA Adducts.** Prior to HPLC analysis, samples were subjected to one-dimensional PEI–cellulose TLC to remove excess [ $\gamma$ -<sup>32</sup>P]ATP and other cofactors. Labeled mixtures were spotted on PEI–cellulose TLC plates (10  $\times$  15 cm) with a paper wick attached and developed overnight with 1 M phosphate buffer (pH 6.8). PEI–cellulose at the origin was removed and extracted four times with 0.5 mL of 4 M pyridinium formate (pH 4.5). Pyridinium formate extracts were combined and evaporated to dryness in a speed-vac. Residues were redissolved in 100  $\mu$ L of 0.3 M sodium phosphate buffer (pH 2.0)/MeOH (90:10 v/v). HPLC analyses of hydrocarbon-modified, <sup>32</sup>P-labeled 3',5'-diphosphodeoxyribonucleosides by HPLC were carried out again using a Shimadzu LC6A liquid chromatograph. Separations were performed on a Zorbax phenyl-modified reverse-phase column (4.6 mm  $\times$  25 cm) with the following solvent system: 0–15 min, a linear gradient of 10–43% B (methanol-buffer A 9:1) in buffer A (0.3 M sodium dihydrogen orthophosphate and 0.2 M orthophosphoric acid, adjusted to pH 2.0); 15–60 min, a linear gradient of 43–46% B in buffer A; and 60–140 min, a linear gradient of 46–80% B in buffer A. The flow rate was constant throughout the gradient, 1.2 mL/min. A 7-methylbenz[*a*]anthracene (7-MeBa) 1,2,3,4-tetrahydrotetraol, which eluted in the shallow part of the gradient, was used as an internal UV marker. DNA adduct levels were estimated essentially as described by Gorelick and Wogan (31). Adduct-associated radioactivity after subtracting background was calculated, taking into account the fraction of the total sample injected and decay of radiolabel from the time of postlabeling. Adduct-associated radioactivity was converted to a molar equivalent amount of adduct, assuming only one <sup>32</sup>P-labeled phosphate group per adduct molecule, and binding levels were expressed as femtomole of adduct per milligram of epidermal DNA.

## Results

**Analysis of DB[a,j]A–DNA Adducts Using [<sup>3</sup>H]-DB[a,j]A.** The total covalent binding of [<sup>3</sup>H]DB[a,j]A to mouse epidermal DNA was determined at the initiating dose of 400 nmol per mouse (6). Based on total DNA-associated radioactivity at this dose, [<sup>3</sup>H]DB[a,j]A bound to epidermal DNA at the level of  $9.92 \pm 1.45$  pmol/mg of DNA (average  $\pm$ SD of three determinations). However, after digestion of isolated DNA samples to deoxyribonucleosides, only  $8.64 \pm 0.4\%$  of the total radioactivity was found in the methanol-soluble material obtained from the short Sephadex LH-20 columns. Thus, the effective level of covalent binding determined using [<sup>3</sup>H]-DB[a,j]A was actually  $0.86 \pm 0.16$  pmol/mg of DNA.

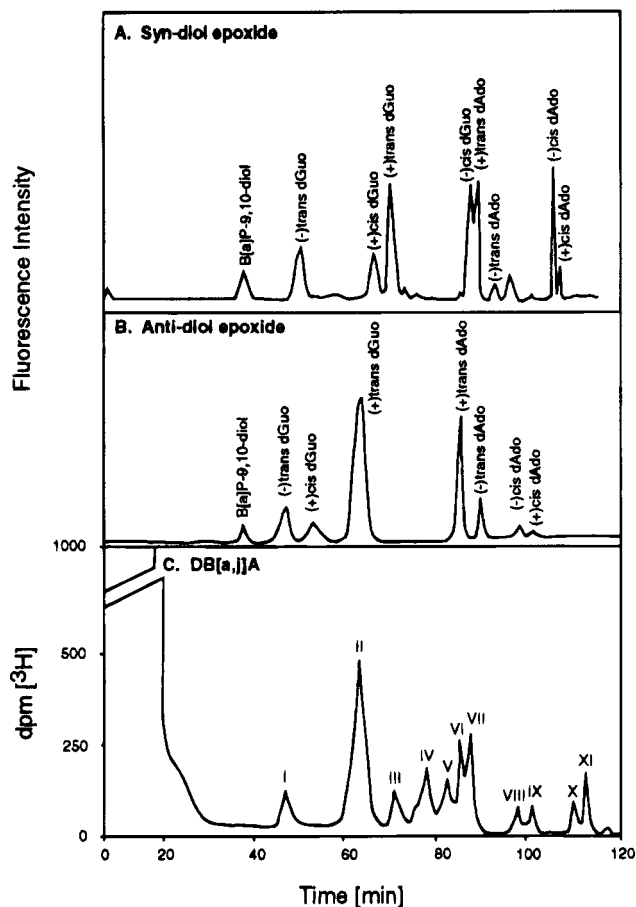


**Figure 1.** HPLC profile of [ $^3\text{H}$ ]DB[*a,j*]A–DNA adducts formed in Sencar mouse epidermis 24 h after application of 400 nmol of [ $^3\text{H}$ ]DB[*a,j*]A (panel C). The sample, containing  $\sim 150\,000$  dpm was injected onto the HPLC column, and immediately after injection 0.5-min fractions were collected. The radioactivity in each fraction is expressed as net dpm after subtraction of background values. The fluorescence profiles (ex 293, em 405) of ( $\pm$ )*anti*-DB[*a,j*]ADE–DNA (panel B) and ( $\pm$ )*syn*-DB[*a,j*]ADE–DNA (panel A) marker adducts co-injected with the radioactive samples are also shown.

Similar results were obtained using either [ $\text{G-}^3\text{H}$ ]DB[*a,j*]A or [ $7\text{-}^3\text{H}$ ]DB[*a,j*]A.

The chromatographic elution profile of methanol-soluble products after enzymatic hydrolysis and purification (on short LH-20 columns) of epidermal DNA isolated from mice treated with [ $^3\text{H}$ ]DB[*a,j*]A is shown in Figure 1, panel C. Individual DNA adduct levels are presented in Table 1 (average of two separate experiments). In order to obtain sufficient amounts of radioactivity in methanol phases for HPLC analyses, it was necessary to pool multiple samples. Generally, samples were pooled from 8–10 groups of mice (80–100 mice total). Eleven radioactive peaks were consistently observed in HPLC chromatograms of these samples (peaks I–XI, Figure 1, panel C). Seven of these peaks were tentatively identified based on cochromatography with marker DNA adducts as follows: peak I, ( $-$ )*anti*-DB[*a,j*]ADE–*trans*-dGuo; peak II, ( $+$ )*anti*-DB[*a,j*]ADE–*trans*-dGuo; peak III, ( $+$ )*syn*-DB[*a,j*]ADE–*trans*-dGuo; peak VI, ( $+$ )*anti*-DB[*a,j*]ADE–*trans*-dAdo; peak VIII, ( $-$ )*anti*-DB[*a,j*]ADE–*cis*-dAdo; peak IX, ( $+$ )*anti*-DB[*a,j*]ADE–*cis*-dAdo, and peak XI, DB[*a,j*]A–5,6-oxide–dAdo. The identity of peak VII [( $+$ )*syn-trans*-dAdo–( $-$ )*syn-cis*-dGuo] remains ambiguous at present since more than one marker DNA adduct (as noted) elutes coincident with this peak. Finally, the unidentified peaks in the chromatogram shown in Figure

**Table 1.** Formation of Individual DB[*a,j*]A–DNA Adducts in Mouse Epidermis after Topical Application of [ $^3\text{H}$ ]DB[*a,j*]A

HPLC peaks	tentative identity of peaks	fmol of adduct/mg of DNA <sup>a</sup>	% of total radioactivity <sup>b</sup>
fractions 1–50	solvent front		84.53
I	( $-$ ) <i>anti</i> -DB[ <i>a,j</i> ]ADE– <i>trans</i> -dGuo	4.04	0.47
II	( $+$ ) <i>anti</i> -DB[ <i>a,j</i> ]ADE– <i>trans</i> -dGuo	24.08	2.80
III	( $+$ ) <i>syn</i> -DB[ <i>a,j</i> ]ADE– <i>trans</i> -dGuo	4.56	0.53
IV	unknown	6.97	0.81
V	unknown	5.50	0.64
VI	( $+$ ) <i>anti</i> -DB[ <i>a,j</i> ]ADE– <i>trans</i> -dAdo	6.10	0.71
VII	( $+$ ) <i>syn</i> -DB[ <i>a,j</i> ]ADE– <i>trans</i> -dAdo/ ( $-$ ) <i>syn</i> -DB[ <i>a,j</i> ]ADE– <i>cis</i> -dGuo	7.05	0.82
VIII	( $-$ ) <i>anti</i> -DB[ <i>a,j</i> ]ADE– <i>cis</i> -dAdo	2.32	0.27
IX	( $+$ ) <i>anti</i> -DB[ <i>a,j</i> ]ADE– <i>cis</i> -dAdo	1.81	0.21
X	unknown	2.49	0.29
XI	( $\pm$ )DB[ <i>a,j</i> ]A 5,6-oxide–dAdo	2.32	0.27

<sup>a</sup> Values in the table are expressed as fmol of adduct/mg of epidermal DNA and represent an average of two separate experiments. Maximum variation between the two experiments was 15%. Recovery from the HPLC column was  $\geq 90\%$  for both samples. <sup>b</sup> Percentage (%) of total radioactivity eluted from HPLC column.

1 (peaks IV, V, and X) did not cochromatograph with any of the marker DNA adducts prepared from ( $+$ ) or ( $-$ )*anti*-DB[*a,j*]ADE, ( $\pm$ )*syn*-DB[*a,j*]ADE, or ( $\pm$ )DB[*a,j*]A–5,6-oxide. Note that the positions of DB[*a,j*]A 5,6-oxide DNA adduct markers where they elute in the current HPLC system are not shown in Figure 1. The relative positions of both the 5,6-oxide dGuo and dAdo adducts can be found in ref 10. Nevertheless, the tentative identification of DB[*a,j*]A 5,6-oxide DNA adduct in the present study is based on cochromatography with these marker adducts.

Examination of the representative HPLC profile in Figure 1 revealed considerable radioactivity in the early, more polar portion of the chromatogram. This finding was typical of all DB[*a,j*]A–DNA adduct samples obtained in the present study regardless of the source or nature of the [ $^3\text{H}$ ]DB[*a,j*]A used (i.e., [ $\text{G-}^3\text{H}$ ]DB[*a,j*]A or [ $7\text{-}^3\text{H}$ ]DB[*a,j*]A). The consistent presence of this early eluting radioactive material as well as the large fraction of DNA-associated radioactivity eluting in the water phases from the LH-20 cleanup step raised several questions about the nature of this material. First, this material could be due to incomplete hydrolysis of DNA samples. This possibility was partially excluded by rechromatography of pooled fractions 1–40 after additional enzymatic digestion. This material again eluted in the first 30 fractions of the HPLC chromatogram. A second possibility for this early eluting material was the presence of early eluting polar DNA adducts. This latter possibility was further explored by  $^{32}\text{P}$ -postlabeling analysis as described below.

**Analysis of DB[*a,j*]A–DNA Adducts Using  $^{32}\text{P}$ -Postlabeling.** To further examine the DB[*a,j*]A–DNA adducts formed in mouse epidermis in the present study, we used as a second approach a  $^{32}\text{P}$ -postlabeling technique coupled with HPLC analysis of adducted 3',5'-diphosphodeoxyribonucleosides. For these experiments, the DNA samples were isolated from mouse skin that had been treated with either DB[*a,j*]A, DB[*a,j*]A *trans*-3,4-diol, or the bay-region *anti*- or *syn*-3,4-diol 1,2-epoxides of DB[*a,j*]A. Following hydrolysis, samples were  $^{32}\text{P}$ -postlabeled and examined by HPLC using a phenyl-modified Zorbax column (see Materials and Methods).

In our initial studies using the  $^{32}\text{P}$ -postlabeling approach, we prepared marker adducts from the ( $\pm$ )*anti*-

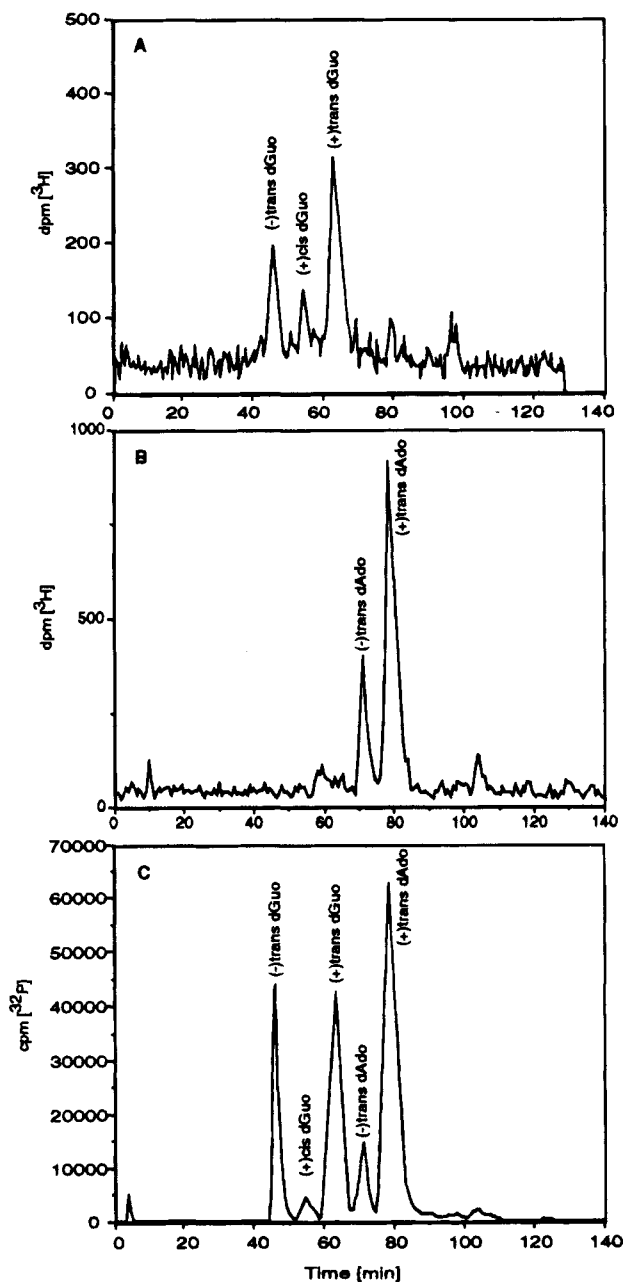


**Figure 2.** HPLC profiles of 3',5'-diphosphodeoxyribonucleoside adducts obtained from reactions of [ $^3\text{H}$ ]dGuo (panel A) or [ $^3\text{H}$ ]dAdo (panel B) labeled or unlabeled (panel C) calf thymus DNA with ( $\pm$ )*anti*-DB[a,j]ADE. Following reactions, adduct DNA samples were enzymatically digested and subsequently postlabeled with cold ATP (panels A and B) or [ $^{32}\text{P}$ ]ATP (panel C) as described in Materials and Methods. The identities of the dGuo and dAdo peaks in panels A and B were determined after hydrolysis of pooled HPLC peaks to deoxyribonucleosides and cochromatography with DNA adduct markers as described in Figure 1.

DB[a,j]A 3,4-diol 1,2-epoxide. This was accomplished by digesting [ $^3\text{H}$ ]dGuo or [ $^3\text{H}$ ]dAdo containing calf thymus DNA that had been reacted with the diol epoxide as previously described (10) followed by postlabeling with unlabeled ATP as described in Materials and Methods. Representative HPLC chromatograms of these samples are shown in Figure 2 (panels A and B, respectively) as well as the profile of  $^{32}\text{P}$ -postlabeled adducts obtained from reaction of the ( $\pm$ )*anti*-diol epoxide with unlabeled calf thymus DNA (Figure 2, panel C). Panel A of Figure 2 shows the retention characteristics of the 3',5'-diphosphodeoxyribonucleoside adducts containing [ $^3\text{H}$ ]dGuo in

the HPLC system employed. Three DNA adduct peaks corresponding to the ( $-$ )*trans*-, ( $+$ )*cis*-, and ( $+$ )*trans*-dGuo adducts were routinely observed with an elution order similar to the profile obtained when analyzing the deoxyribonucleoside adducts (see Figure 1, panel B). Panel B of Figure 2 shows the retention characteristics of the 3',5'-diphosphodeoxyribonucleosides containing [ $^3\text{H}$ ]dAdo in the HPLC system employed. Two DNA adduct peaks were routinely observed in these chromatograms: ( $-$ )*trans*- and ( $+$ )*trans*-dAdo. The ( $+$ )*cis*- and ( $-$ )*cis*-dAdo addition products were not readily detected under the experimental conditions employed. Furthermore, in contrast to the results obtained with the [ $^3\text{H}$ ]dGuo-labeled 3',5'-diphosphodeoxyribonucleoside adducts, the relative retention characteristics of the [ $^3\text{H}$ ]dAdo-labeled 3',5'-diphosphodeoxyribonucleoside adducts were different than those of the corresponding deoxyribonucleoside adducts (see again panel B of Figure 1). In this regard, the ( $-$ )*trans*-dAdo adduct eluted prior to the ( $+$ )*trans*-dAdo adduct compared to the reverse elution order for the deoxyribonucleoside adducts. Panel C of Figure 2 shows the profile of ( $\pm$ )*anti*-DB[a,j]ADE adducts following  $^{32}\text{P}$ -postlabeling analysis of an unlabeled calf thymus DNA sample that had been reacted with the diol epoxide. It should be readily apparent which peaks in panel C correspond to dGuo (panel A) and dAdo (panel B) adducts. Another important observation from panel C of Figure 2 is that the ratio of ( $+$ )*anti*-DB[a,j]ADE-*trans*-dGuo to ( $+$ )*anti*-DB[a,j]ADE-dAdo was consistently lower in analyses using  $^{32}\text{P}$ -postlabeling compared to the results obtained upon analysis of deoxyribonucleoside adducts as shown in Figure 1 (see Figure 1, panel B).

Figure 3 shows the HPLC elution profiles of the  $^{32}\text{P}$ -postlabeled 3',5'-diphosphodeoxyribonucleoside adducts obtained following topical application of DB[a,j]A (panel A), ( $\pm$ )DB[a,j]A *trans*-3,4-diol (panel B), ( $\pm$ )*anti*-DB[a,j]ADE (panel C), and ( $\pm$ )*syn*-DB[a,j]ADE (panel D) to Sencar mouse epidermis. The extent of DNA modification determined by the  $^{32}\text{P}$ -postlabeling method was  $0.08 \pm 0.03$ ,  $0.11 \pm 0.03$ , and  $0.21 \pm 0.05$  pmol/mg DNA for the parent compound, ( $\pm$ )DB[a,j]A *trans*-3,4-diol, and ( $\pm$ )*anti*-DB[a,j]ADE, respectively. Thus, the average overall recovery of DB[a,j]A-DNA adducts by HPLC  $^{32}\text{P}$ -postlabeling was only 9% of that determined using [ $^3\text{H}$ ]DB[a,j]A. Individual DNA adduct levels are presented in Tables 2 (DB[a,j]A and ( $\pm$ )DB[a,j]A *trans*-3,4-diol) and 3 (( $\pm$ )*anti*-DB[a,j]ADE). The DNA adduct profiles obtained following topical application of DB[a,j]A and its *trans*-3,4-diol were qualitatively very similar in that 12 and 11 DNA adduct peaks, respectively, were consistently observed. A very late eluting DNA adduct peak (peak XII, Figure 3, panel A) was not observed in the chromatograms of DNA samples from ( $\pm$ )DB[a,j]A *trans*-3,4-diol-treated mice. A striking observation from the data in panels A and B of Figure 3 is the large number and relative quantity of adduct peaks eluting within the first 40 min of the HPLC gradient employed (i.e., early in the chromatogram). As shown in Figure 2 and in panels C and D of Figure 3 (see also below), no ( $\pm$ )*anti*- or ( $\pm$ )*syn*-diol epoxide adducts eluted prior to 40 min in the HPLC gradient system utilized.

To further explore the nature of the DB[a,j]A-DNA adducts formed in mouse epidermal DNA detected by  $^{32}\text{P}$ -postlabeling, we also analyzed the covalent DNA adducts formed after topical application of either ( $\pm$ )*anti*- (Figure 3, panel C) or ( $\pm$ )*syn*-DB[a,j]ADE (Figure 3, panel D). As

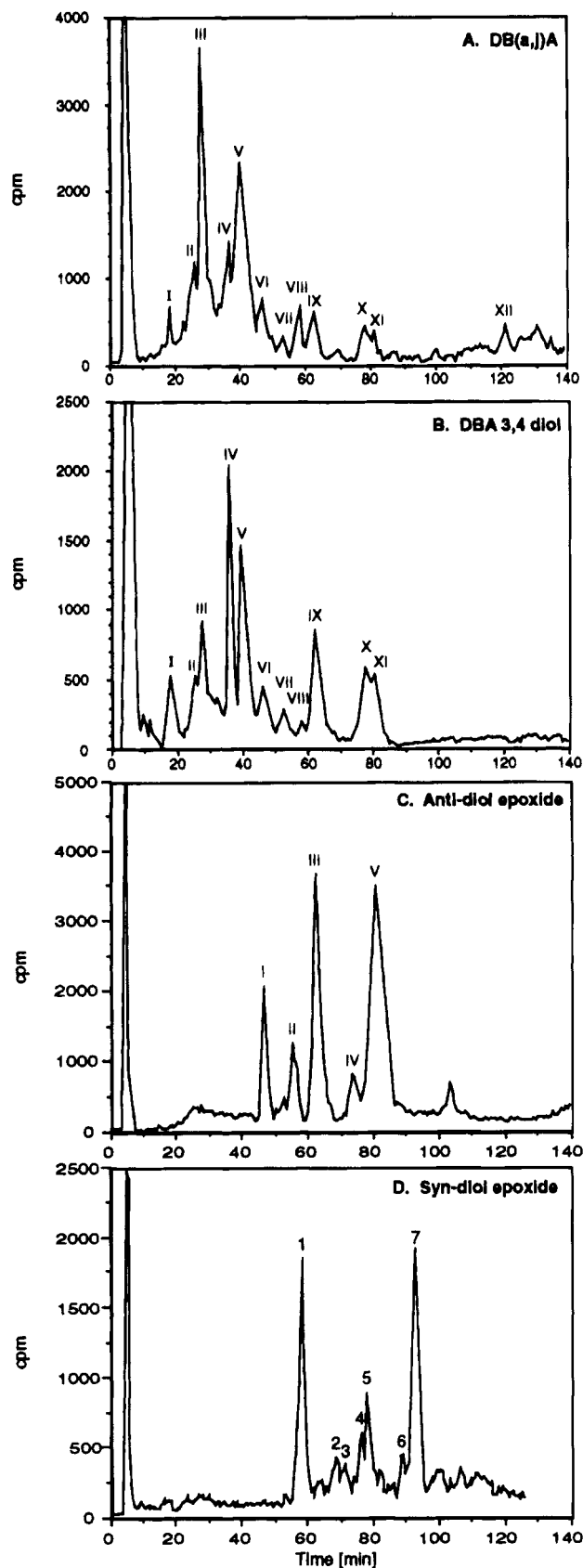


**Figure 3.** HPLC profiles of  $^{32}\text{P}$ -labeled 3',5'-diphosphodeoxyribonucleoside adducts formed in Sencar mouse epidermis 24 h after application of 1600 nmol of DB[a,j]A (panel A) or DB[a,j]A 3,4-diol (panel B) or 3 h after topical application of 400 nmol of ( $\pm$ )*anti*- (panel C) or *syn*-DB[a,j]ADE (panel D). The samples containing about  $\sim 400\,000$  cpm were injected onto the HPLC column, and immediately after injection 0.5-min fractions were collected. The radioactivity is expressed as net cpm after subtraction of background values.

expected, *in vivo* DNA adduct peaks obtained from either diol epoxide eluted after 40 min in the HPLC system employed. The identities of the major DNA adduct peaks present in panel C of Figure 3 are based on cochromatography with the  $^3\text{H}$ -labeled 3',5'-diphosphodeoxyribonucleoside adducts described in Figure 2. In this regard, three peaks derived from reaction with dGuo were present in DNA samples from ( $\pm$ )*anti*-diol epoxide treated mice [corresponding to ( $-$ )*trans*-, ( $-$ )*cis*-, and ( $+$ )*trans*-dGuo]. Two dAdo adduct peaks were also found in these samples corresponding to the ( $+$ )*trans* and ( $-$ )*trans* addition products. Overall the ratio of the ( $+$ )*anti-trans*-dGuo to ( $+$ )*anti-trans*-dAdo adduct was similar to that observed in HPLC profiles obtained after *in vitro* reaction of calf thymus DNA with ( $\pm$ )*anti*-DB[a,j]ADE followed by  $^{32}\text{P}$ -postlabeling (Figure 2, panel C). However, this ratio was again significantly lower than observed after *in vitro* reaction of the diol epoxide with calf thymus DNA followed by analysis of deoxyribonucleoside adducts or following topical application of [ $^3\text{H}$ ]DB[a,j]A to mouse epidermis *in vivo* followed by analysis of deoxyribonucleoside adducts (see again Figure 1). A comparison of appropriate peaks in Tables 1 and 2 shows that the ratio of ( $+$ )*anti*-DB[a,j]ADE-*trans*- $N^2$ -dGuo to ( $+$ )*anti*-DB[a,j]ADE-*trans*- $N^6$ -dAdo adduct estimated by the  $^{32}\text{P}$ -postlabeling method employed in DNA samples from DB[a,j]A and ( $\pm$ )DB[a,j]A *trans*-3,4-diol-treated mice was also lower than estimated by measurement of  $^3\text{H}$ -labeled adducts. This ratio was 1.6 and 2.3 for DB[a,j]A and ( $\pm$ )DB[a,j] 3,4-diol, respectively compared to a ratio of 3.9 for the parent compound as determined with [ $^3\text{H}$ ]DB[a,j]A suggesting lower recovery of the ( $+$ )*anti*-DB[a,j]ADE-*trans*- $N^2$ -dGuo adduct.

The DNA adduct profile obtained from epidermal DNA of ( $\pm$ )*syn*-DB[a,j]ADE-treated mice yielded two major peaks as well as several less abundant DNA adduct peaks. At the present time, these peaks have not been further characterized. However, it should be noted that two  $^{32}\text{P}$ -postlabeled DNA adduct peaks (peaks VIII and X) in the HPLC profiles from DB[a,j]A (Figure 3, panel A) and ( $\pm$ )DB[a,j]A 3,4-diol-treated (Figure 3, panel B) mice consistently co-eluted with  $^{32}\text{P}$ -postlabeled *syn*-diol epoxide DNA adduct peaks formed after topical application of the ( $\pm$ )*syn*-diol epoxide (peaks 1 and 5 in Figure 3, panel D).

Note that the portion of the chromatogram from DB[a,j]A-treated mice corresponding to the diol epoxide adducts (Figure 3, panel A, after 40 min) revealed a profile very similar to that obtained using [ $^3\text{H}$ ]DB[a,j]A (Figure 1, panel C). In this regard, three major *anti*-diol epoxide adducts were tentatively identified, two *syn*-diol epoxide adducts were detected (not further identified), and a very late eluting peak was detected (possibly a 5,6-oxide adduct although not further identified at present). The major difference between the two different sets of data was that the ( $+$ )*anti*- and ( $-$ )*anti*-DB[a,j]ADE-*cis*-dAdo adducts were not detectably present in HPLC chromatograms of  $^{32}\text{P}$ -postlabeled adducts. Furthermore, these two adducts were not detected in DNA samples reacted with ( $\pm$ )*anti*-DB[a,j]ADE *in vitro* (Figure 2, panel C), and therefore it is not surprising that they were not detected in HPLC chromatograms from *in vivo* samples. Possible explanations for the inability to detect these two minor adducts using the current  $^{32}\text{P}$ -postlabeling method are (i) inability to resolve these adducts from other peaks in our HPLC chromatograms and/or (ii) inefficient labeling of these adducts with  $^{32}\text{P}$ .

**Table 2. Relative Levels of DB[a,j]A-DNA Adducts Formed in Mouse Epidermis after Topical Application of DB[a,j]A or DB[a,j] 3,4-Diol and Determined by HPLC <sup>32</sup>P-Postlabeling**

HPLC peaks	tentative identity of peaks	DB[a,j]A		DB[a,j] 3,4-diol	
		fmol of adduct/ mg of DNA <sup>a</sup>	% of total radioactivity <sup>b</sup>	fmol of adduct/ mg of DNA <sup>a</sup>	% of total radioactivity <sup>b</sup>
fractions 1-10	solvent front		47.85		66.20
I	unknown	1.24	1.55	1.36	1.24
II	unknown	2.72	3.40	1.63	1.48
III	unknown	7.68	9.60	2.87	2.06
IV	unknown	2.31	2.89	4.49	4.08
V	unknown	8.28	10.35	4.68	4.25
VI	(-) <i>anti</i> -DB[a,j]ADE- <i>trans</i> -dGuo	1.48	1.85	1.80	1.64
VII	unknown	0.94	1.18	1.13	1.03
VIII	<i>syn</i> -DB[a,j]ADE adduct	1.38	1.73	0.55	0.50
IX	(+) <i>anti</i> -DB[a,j]ADE- <i>trans</i> -dGuo	1.71	2.14	3.85	3.50
X	<i>syn</i> -DB[a,j]ADE adduct	1.59	1.99	2.07	1.88
XI	(+) <i>anti</i> -DB[a,j]ADE- <i>trans</i> -dAdo	1.05	1.32	1.69	1.54
XII	unknown	1.70	2.13		

<sup>a</sup> Values in the table are expressed as fmol of adduct/mg of epidermal DNA and represent an average of two separate experiments with maximum variation of 18%. The values are based on total radioactivity eluted from the HPLC column after subtracting background as described in Materials and Methods. <sup>b</sup> Percentage (%) of total radioactivity eluted from HPLC columns.

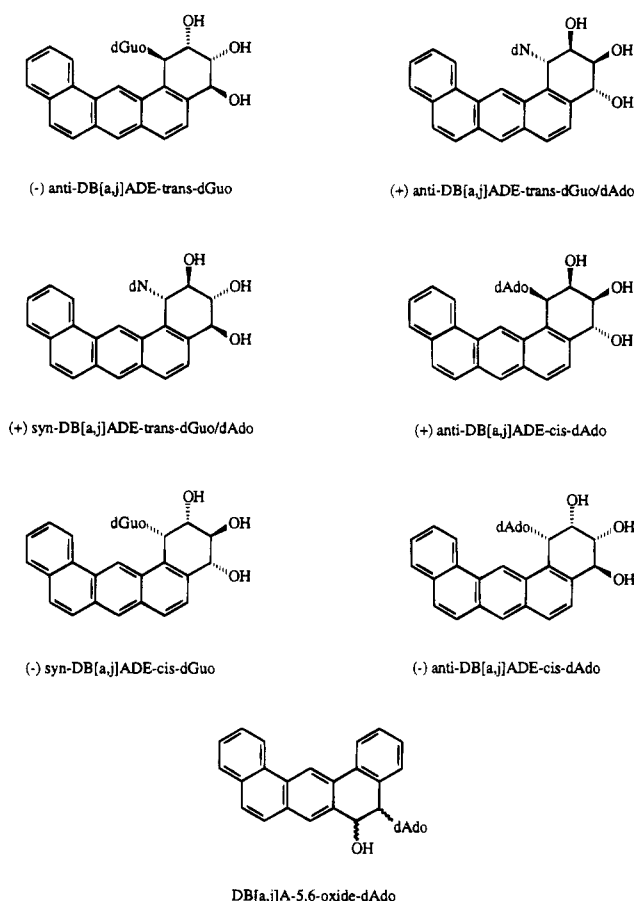
**Table 3. Relative Levels of (±)*anti*-DB[a,j]ADE-DNA Adducts Formed in Vivo As Determined by HPLC <sup>32</sup>P-Postlabeling**

HPLC peaks	tentative identity of peaks	fmol adduct/ mg of DNA <sup>a</sup>	% of total radio- activity <sup>b</sup>
fractions 1-10	solvent front		18.49
I	(-) <i>anti</i> -DB[a,j]ADE- <i>trans</i> -dGuo	9.30	4.43
II	(+) <i>anti</i> -DB[a,j]ADE- <i>cis</i> -dGuo	6.32	3.01
III	(+) <i>anti</i> -DB[a,j]ADE- <i>trans</i> -dGuo	33.37	15.89
IV	(-) <i>anti</i> -DB[a,j]ADE- <i>trans</i> -dAdo	5.25	2.50
V	(+) <i>anti</i> -DB[a,j]ADE- <i>trans</i> -dAdo	75.45	35.93

<sup>a</sup> Values in the table are expressed as fmol of adduct/mg of epidermal DNA and represent an average of two separate experiments with maximum variation of 18%. The values are based on total radioactivity eluted from HPLC columns after subtracting background as described in Materials and Methods. <sup>b</sup> Percentage (%) of total radioactivity eluted from HPLC columns.

## Discussion

The present study has examined the DNA adducts formed in mouse epidermis after topical application of [<sup>3</sup>H]DB[a,j]A or after topical application of unlabeled DB[a,j]A and its derivatives followed by <sup>32</sup>P-postlabeling. The bay-region theory predicts that the metabolic activation of DB[a,j]A would proceed through the formation of 3,4-diol 1,2-epoxide metabolites (7). The high tumor-initiating activity of (±)*anti*-DB[a,j]ADE relative to the parent hydrocarbon provides support for this hypothesis (6). Analysis of DNA adducts formed in mouse epidermis, 24 h after topical treatment with [<sup>3</sup>H]DB[a,j]A, revealed the presence of the DNA adducts formed from the *anti*-DB[a,j]ADE and in particular the (+)*anti*-DB[a,j]ADE (see Table 1; Figure 1, panel C; and Chart 1). Interestingly, the major DNA adduct formed from the (+)*anti*-DB[a,j]ADE in mouse epidermis as assessed following topical application of [<sup>3</sup>H]DB[a,j]A was tentatively identified as the (+)*anti*-DB[a,j]ADE-*trans*-N<sup>2</sup>-dGuo. This diol epoxide isomer has the (4*R*,3*S*)-diol (2*S*,1*R*)-epoxide absolute configuration (8, 9); the configuration which has been shown to be the most tumorigenic of the corresponding four configurational isomers of bay-region diol epoxides derived from B[a]P, chrysene, benz[*a*]anthracene, and B[c]Ph (32, 33). In previous studies of the in vitro reactions of (±)*anti*-DB[a,j]ADE with calf thymus DNA, we observed considerable modification of dAdo residues (~25% of the adducts were with dAdo) (8). After topical application of [<sup>3</sup>H]DB[a,j]A to mouse epidermis, two dAdo adducts were tentatively identified as arising from the

**Chart 1. Chemical Structures of DNA Adducts Derived from *anti*-Diol Epoxide, *syn*-Diol Epoxide, and 5,6-Oxide of DB[a,j]A Formed in Vivo<sup>a</sup>**

(+)*anti*-diol epoxide (both the *cis* and *trans* addition products) (see Figure 1, Table 1, and Chart 1). Similar to our results with in vitro reactions, the dGuo adducts formed from the (±)*anti*-diol epoxide of DB[a,j]A in mouse skin were also present in higher proportion than the corresponding dAdo adducts. For example, the ratio of (+)*anti*-DB[a,j]ADE-*trans*-dGuo to (+)*anti*-DB[a,j]ADE-*trans*-dAdo was 3.9 (see again Table 1). Thus, the relative proportions of dGuo vs dAdo adducts formed in vivo from the *anti*-diol epoxide after topical application of [<sup>3</sup>H]DB[a,j]A was very similar to that observed in in vitro reactions.

It is also interesting that several DNA adduct peaks were tentatively identified as arising from the *syn*-diol epoxide of DB[a,j]A (see again Table 1, Figure 1, and Chart 1). Although the potential tumor-initiating activity of this diol epoxide has not been reported, it is possible that these adducts also contribute to the biological activity of DB[a,j]A. This statement is based on the structural similarity between DB[a,j]A and B[c]Ph. To date, B[c]Ph is the only PAH, whose bay-region *syn*-diol epoxide possesses tumor-initiating activity similar to that of the bay-region *anti*-diol epoxide (33). With this PAH, both the *anti*- and *syn*-diol epoxides are more potent than the parent hydrocarbon. As already noted, the *anti*-diol epoxide of DB[a,j]A is also a more potent tumor initiator than the parent hydrocarbon. Like ( $\pm$ )*anti*-DB[a,j]ADE, the reaction of ( $\pm$ )*syn*-DB[a,j]ADE with calf thymus DNA in vitro yielded higher proportions of dGuo vs dAdo adducts (9, 10). However, due to the ambiguity in identifying peak VII in DNA adduct samples from [ $^3$ H]-DB[a,j]A-treated mice (Figure 1), the exact proportion of *syn*-DB[a,j]ADE-dGuo vs -dAdo adducts formed in vivo could not be accurately determined in the present study.

During the course of our analyses using [ $^3$ H]DB[a,j]A, we consistently noted several late eluting DNA adduct peaks in HPLC chromatograms. To explore the nature of these peaks, we synthesized the K-region 5,6-oxide of DB[a,j]A with the knowledge that K-region oxide adducts of other hydrocarbons are known to elute after the diol epoxide adducts on Sephadex LH-20 or reverse-phase HPLC columns (34, 35). We tentatively identified a dAdo adduct formed with the 5,6-oxide of DB[a,j]A. While the site of reaction on the epoxide ring of DB[a,j]A 5,6-oxide is unknown, molecular orbital (MO) theoretical methods predict greater reactivity in the C-5 ring position. Thus, MO calculations based on the perturbational method of Dewar show reactivity numbers ( $N_i$ ) for the C-5 and C-6 positions of DB[a,j]A 5,6-oxide to be 1.71 and 1.66, respectively; the related  $DE_{\text{deloc}}$  energies are 0.570b and 0.582b, respectively (36). Based solely on these electronic considerations, the reaction may be predicted to take place preferentially in the C-5 ring position. Unfortunately, the amount of material available from the present experiments was insufficient to determine the validity of this prediction. Furthermore, determination of the enantiomeric nature of this K-region oxide-dAdo adduct must await resolution of the (+) and (-) isomers of the 5,6-oxide.

As in our previous studies using mouse keratinocytes in culture (10), comparison of the extent of DNA binding estimated by the measurement of incorporated [ $^3$ H]DB[a,j]A and the radioactivity eluted in the course of adduct separation on Sephadex LH-20 columns revealed a significant loss of radioactive material during this cleanup procedure. A similar behavior, although not to such an extent was previously reported for DNA binding experiments with [ $^3$ H]benzo[a]pyrene (37, 38) and [ $^7$ - $^3$ H]MeBA (39). We have found that most radioactivity in the water phases following LH-20 chromatography of [ $^3$ H]DB[a,j]A-DNA adduct samples was associated with normal deoxyribonucleosides and nucleotides (10, 40).<sup>2</sup> Again, this was the case whether [ $G$ - $^3$ H]- or [ $^7$ - $^3$ H]DB[a,j]A was used. In addition, HPLC analysis of [ $^3$ H]DB[a,j]A-DNA adducts revealed considerable amount of radioactivity in the more polar portion of these chromatograms (see

Figure 1, panel C). A major finding of the present study was the presence of highly polar DB[a,j]A-DNA adducts not retained on reversed-phase columns using conventional methodology (i.e., separation of the hydrocarbon-deoxyribonucleoside adducts).

The existence of highly polar PAH-DNA adducts was recently shown for another isomer of DBA, DB[a,h]A (41), as well as for several other PAH (42, 43). The existence of highly polar DNA adducts in epidermal DNA samples from DB[a,j]A-treated mice was verified through use of a  $^{32}$ P-postlabeling technique coupled with HPLC. Chromatography was carried out using a phenyl-modified reverse-phase column and sample elution with a low pH, phosphate buffer gradient in methanol. A similar HPLC system was successfully used in resolving 3',5'-diphosphodeoxyribonucleoside adducts derived from DB[a,h]A and benzo[b]fluoranthene (reviewed in ref 44). This method, in addition to being highly sensitive, also facilitated partial resolution of more polar DB[a,j]A-DNA adducts. Thus, HPLC profiles of 3'-diphosphodeoxyribonucleoside adducts obtained from epidermal DNA isolated from mice treated with the parent compound DB[a,j]A or its *trans*-3,4-diol revealed 12 or 11 different adduct peaks, respectively.

Notably, approximately half of these DNA adduct peaks in each case (peaks I-V) eluted prior to standard *anti*- and *syn*-diol epoxide DNA adduct peaks. The exact identity of these early eluting adducts remains unknown at present. In the case of DB[a,h]A, it was reported that the major DNA adduct, one of 10 adducts separated, was derived from the 3,4,10,11-bis-diol. It was postulated that a bis-diol epoxide of the bay-region type may represent the DNA binding species involved (45). In our previous studies on metabolism of DB[a,j]A in mouse keratinocytes cultures, we did not establish formation of bis-dihydrodiol metabolites, but several early eluting metabolites were found in HPLC chromatograms of organic extracts from cultures exposed to DB[a,j]A (46). However, an earlier study of the metabolism of DB[a,j]A by rat liver microsomes reported the presence of bis-dihydrodiol metabolites (47). In the current study, the observation that the early eluting DB[a,j]A-DNA adducts had retention times identical to early eluting DNA adducts formed after topical application of DB[a,j]A 3,4-diol indirectly supports the hypothesis that bis-dihydrodiol epoxide metabolites could account for at least some of the early eluting DNA adducts we observed. Definite proof of the nature of the polar adducts formed in mouse epidermis after application of DB[a,j]A must await synthesis and physico-chemical characterization of bis or phenol-diol epoxides and their resultant DNA adducts.

Another important aspect of our current study using the  $^{32}$ P-postlabeling method involved quantitation. In this regard, the average overall level of  $^{32}$ P-postlabeled adducts for the parent compound, DB[a,j]A, was only 9% of that obtained when calculated using [ $^3$ H]DB[a,j]A. These results are similar to those reported for several other PAH. For example Mlcoch et al. (48) reported that the calculated DNA binding yield of dibenz[a,h]anthracene (DB[a,h]A) using the  $^{32}$ P-postlabeling method was only 34% of the binding yield calculated from the amount of radioactivity recovered in the DNA modified with [ $^{14}$ C]DB[a,h]A. Gorelick and Wogan (31) also reported that recovery of fluoranthene (FA) adducts by  $^{32}$ P-postlabeling constituted only 10-15% of total DNA binding for FA determined following exposure to [ $^3$ H]FA.

<sup>2</sup> W. Baer-Dubowska, R. V. Nair, and J. DiGiovanni, unpublished studies.

Finally, Segerbäck and Vodicka (49) showed that, in general, recoveries of PAH adducts by the  $^{32}\text{P}$ -postlabeling method were lower (range 3–60%) than that estimated by  $^3\text{H}$ -labeled compounds for 10 different PAH. In the present study, we also observed differences in recovery of individual adducts of DB[a,j]A. In this regard, the recovery of the (+)anti-DB[a,j]ADE-trans- $\text{N}^2$ -dGuo adduct was consistently lower (as assessed by the ratio of this adduct to the (+)anti-DB[a,j]ADE-trans- $\text{N}^6$ -dAdo adduct) in samples analyzed by  $^{32}\text{P}$ -postlabeling compared to samples analyzed following application of [ $^3\text{H}$ ]DB[a,j]A. Detailed information regarding individual adduct recoveries by the  $^{32}\text{P}$ -postlabeling technique is generally lacking. However, Hemminki et al. (50) have reported that the labeling efficiency of the synthetically prepared (+)-anti-benzo[a]pyrene diol epoxide- $\text{N}^2$ -dGuo adduct was only 20%. While further work is necessary, our current data indicate that the recovery of individual adducts by the  $^{32}\text{P}$ -postlabeling method may differ significantly for a given compound.

In conclusion, HPLC analysis of  $^3\text{H}$ -labeled deoxyribonucleoside adducts or  $^{32}\text{P}$ -postlabeled 3',5'-diphosphodeoxyribonucleoside adducts formed following topical application of DB[a,j]A to mouse skin confirmed the formation of both dGuo and dAdo adducts with both anti- and syn-diol epoxides. The major adducts formed from bay-region diol epoxides and K-region epoxides that were tentatively identified are shown in Chart 1. The biological significance of dAdo vs dGuo adducts is still unclear, although it has been suggested that binding to dAdo may be critical for the tumor-initiating activity of some PAH (12, 17, 25). Studies on the nature of point mutations in the c-Ha-ras gene from skin papillomas produced by initiation with DB[a,j]A or ( $\pm$ )anti-DB[a,j]ADE showed that in both cases the dominant mutation was an A $^{182}$   $\rightarrow$  T transversion in codon 61 (18). Based on the available data, we can conclude that dAdo adducts derived from trans addition of the  $\text{N}^6$  of dAdo with the anti-DB[a,j]ADE contribute to the initiating activity of DB[a,j]A. However, at present we cannot exclude the involvement of syn-DB[a,j]ADE-dAdo adducts or more polar dAdo adducts (possibly derived from bis-dihydrodiol epoxides) in the tumor-initiating activity of this PAH. Overall, our current results show that several routes of activation to DNA binding intermediates are potentially possible for DB[a,j]A. One pathway involves the formation of simple epoxides of the K-region type. A second pathway involves bay-region diol epoxides, and a third pathway involves the formation of more polar metabolites, possibly phenol- or bis-dihydrodiol epoxides. The relative importance of each pathway remains to be determined, and studies to address these questions are currently in progress in our laboratory.

**Acknowledgment.** The authors wish to thank Yolanda C. Valderrama for her skills in preparing this manuscript for publication. This research was supported by HSPHS grants (CA36979 (J.D.) and ES04732 (R.G.H.) and American Cancer Society grants FRA-375 (J.D.) and CN-22 (R.G.H.). A portion of this work was presented at the 85th Annual Meeting of the American Association for Cancer Research (Abstract 671) held in San Francisco, CA, in April 1994.

## References

- Miller, E. C. (1978) Some current perspectives on chemical carcinogenesis in humans and experimental animals: presidential address. *Cancer Res.* **38**, 1479–1496.
- Phillips, D. H., and Sims, P. (1979) Polycyclic aromatic hydrocarbon metabolites: Their reactions with nucleic acids. In *Chemical Carcinogens and DNA* (Grover, P. L., Ed.) Vol. 11, pp 29–57, CRC Press, Inc., Boca Raton, FL.
- Sims, P. (1980) The metabolic activation of chemical carcinogens. *Br. Med. Bull.* **36**, 11–18.
- Andrews, A. W., Thibault, L. H., and Lijinsky, W. (1978) The relationship between carcinogenicity and mutagenicity of some polynuclear hydrocarbons. *Mutat. Res.* **51**, 311–318.
- Lijinsky, W., Garcia, H., and Saffiotti, U. (1970) Structure-activity relationship among some polynuclear hydrocarbons and their hydrogenated derivatives. *J. Natl. Cancer Inst.* **44**, 641–649.
- Sawyer, T. W., Baer-Dubowska, W., Chang, K., Crysyp, S. B., Harvey, R. G., and DiGiovanni, J. (1988) Tumor-initiating activity of the bay-region dihydrodiols and diol epoxides of dibenz[a,j]anthracene and cholanthrene on mouse skin. *Carcinogenesis* **9**, 2203–2207.
- Lehr, R. E., Kumar, S., Levin, W., Wood, A. W., Chang, R. L., Conney, A. H., Yagi, H., Sayer, J. M., and Jerina, D. M. (1985) The bay region theory of polycyclic aromatic hydrocarbon carcinogenesis. In *Polycyclic Hydrocarbons and Carcinogenesis* (Harvey, R. G., Ed.) pp 63–84, American Chemical Society, Washington, DC.
- Nair, R. V., Gill, R. D., Cortez, C., Harvey, R. G., and DiGiovanni, J. (1989) Characterization of DNA adducts derived from ( $\pm$ )-trans-3,4-dihydroxy-anti-1,2-epoxy-1,2,3,4-tetrahydrodibenz[a,j]anthracene and ( $\pm$ )-7-methyl-trans-3,4-dihydroxy-anti-1,2-epoxy-1,2,3,4-tetrahydrodibenz[a,j]anthracene. *Chem. Res. Toxicol.* **2**, 341–348.
- Chadha, A., Sayer, J. M., Yeh, H. J. C., Yagi, H., Cheh, A. M., Pannel, L. K., and Jerina, D. M. (1989) Structures of covalent nucleoside adducts formed from adenine, guanine and cytosine bases of DNA and the optically active bay-region 3,4-diol-1,2-epoxides of dibenz[a,j]anthracene. *J. Am. Chem. Soc.* **111**, 5456–5463.
- Nair, R. V., Gill, R. D., Nettikumara, A. N., Baer-Dubowska, W., Cortez, C., Harvey, R. G., and DiGiovanni, J. (1991) Characterization of covalently modified deoxyribonucleosides formed from dibenz[a,j]anthracene in primary cultures of mouse keratinocytes. *Chem. Res. Toxicol.* **4**, 115–122.
- Baird, W. M., and Pruess-Schwartz, D. (1988) Polycyclic aromatic hydrocarbon DNA adducts and their analysis: A powerful technique for characterization of pathways of metabolic activation of hydrocarbons to ultimate carcinogenic metabolites. In *Polycyclic Aromatic Hydrocarbon Carcinogens: Structure-Activity Relationship* (Yang, S. K., and Silverman, B. D., Eds.), Vol. II, pp 141–179, CRC Press, Inc., Boca Raton, FL.
- Dipple, A., Moschel, R. C., and Bigger, C. A. H. (1984) Polynuclear aromatic hydrocarbon. In *Chemical Carcinogenesis* (Searle, C. E., Ed.) Vol. 1, pp 41–163, ASC Monograph 182, American Chemical Society, Washington, DC.
- Dipple, A., Pigott, M., Moschel, R. C., and Constantino, N. (1983) Evidence that binding of 7,12-dimethylbenz[a]anthracene to DNA in mouse embryo cell cultures results in extensive substitution of both adenine and guanine residues. *Cancer Res.* **43**, 4132–4135.
- Pruess-Schwartz, D., Baird, W. M., Yagi, H., Jenna, D. M., Pigott, M. A., and Dipple, A. (1987) Stereochemical specificity in the metabolic activation of benzo[c]phenanthrene to metabolites that covalently bind to DNA in rodent embryo cell cultures. *Cancer Res.* **47**, 4032–4037.
- Dipple, A., Pigott, M. A., Agarwal, S. K., Yagi, H., Sayer, J. M., and Jerina, D. M. (1987) Optically active benzo[c]phenanthrene diol epoxides bind extensively to adenine in DNA. *Nature* **327**, 535–536.
- Szeliga, J., Lee, H., Harvey, R. G., and Dipple, A. (1994) Reaction with DNA and mutagenic specificity of syn-benzo[g]chrysene 11,12-dihydrodiol 13,14-epoxide. *Chem. Res. Toxicol.* **7**, 420–427.
- Szeliga, J., Hilton, B. D., Lee, H., Harvey, R. G., and Dipple, A. (1994) DNA adducts formed by syn dihydrodiol epoxides of polycyclic aromatic hydrocarbons. *Polycyclic Aromat. Compd.* **6**, 87–93.
- Gill, R. D., Beltran, L., Nettikumara, A. N., Harvey, R. G., Kootstra, A., and DiGiovanni, J. (1992) Analysis of point mutations in murine c-Ha-ras of skin tumors initiated with dibenz[a,j]anthracene and derivatives. *Mol. Carcinog.* **6**, 53–59.
- Reddy, M. V., Gupta, R. C., and Randerath, K. (1981)  $^{32}\text{P}$ -base analysis of DNA. *Anal. Biochem.* **117**, 271–279.
- Harvey, R. G., Cortez, C., and Jacobs, S. A. (1982) Synthesis of polycyclic aromatic hydrocarbons via a novel annelation method. *J. Org. Chem.* **47**, 2120–2125.
- Harvey, R. G., Cortez, C., Sawyer, T. W., and DiGiovanni, J. (1988) Synthesis of the tumorigenic 3,4-dihydrodiol metabolites of dibenz[a,j]anthracene and 7,14-dimethyl-dibenz[a,j]anthracene. *J. Med. Chem.* **31**, 1308–1312.

- (22) Harvey, R. G., Goh, S. H., and Cortez, C. (1975) K-region oxides and related oxidized metabolites of carcinogenic aromatic hydrocarbons. *J. Am. Chem. Soc.* **97**, 3468-3479.
- (23) Harvey, R. G., Pataki, J., and Lee, H. (1986) Synthesis of dihydrodiol and diol epoxide metabolites of chrysene and 5-methylchrysene. *J. Org. Chem.* **51**, 1407-1412.
- (24) Ittah, Y., Thakker, D. R., Levin, W., Croisy-Delcey, M., Ryan, D. E., Thomas, P. E., Conney, A. H., and Jerina, D. M. (1983) Metabolism of benz[*c*]phenanthrene by rat liver microsomes and by a purified monooxygenase system reconstituted with different isozymes of cytochrome P-450. *Chem. Biol. Interact.* **45**, 15-28.
- (25) DiGiovanni, J., Fisher, E. F., Aalfs, K. K., and Prichett, W. P. (1985) Covalent binding of 7,12-dimethylbenz[*a*]anthracene and 10-fluoro-7,12-dimethylbenz[*a*]anthracene to mouse epidermal DNA and its relationship to tumor-initiating activity. *Cancer Res.* **45**, 591-597.
- (26) DiGiovanni, J., Decina, P. C., Prichett, W. P., Fisher, E. P., and Aalfs, K. (1985) Formation and disappearance of benzo[*a*]pyrene DNA-adducts in mouse epidermis. *Carcinogenesis* **6**, 741-747.
- (27) Ashurst, S. W., Cohen, G. M., Nesnow, S., DiGiovanni, J., and Slaga, T. J. (1983) Formation of benzo[*a*]pyrene/DNA adducts and their relationship to tumor initiation in mouse epidermis. *Cancer Res.* **43**, 1024-1029.
- (28) Baer-Dubowska, W., Morris, R. J., Gill, R. D., and DiGiovanni, J. (1990) Distribution of covalent DNA adducts in mouse epidermal subpopulations after topical application of benzo[*a*]pyrene and 7,12-dimethylbenz[*a*]anthracene. *Cancer Res.* **50**, 3048-3054.
- (29) Moller, L., Zeisig, M., and Vodicka, P. (1993) Optimization of an HPLC method for analyses of <sup>32</sup>P-postlabeled DNA adducts. *Carcinogenesis* **14**, 1343-1348.
- (30) Jones, N. J., Kadhim, M. A., Hoskons, P. L., Parry, J. M., and Waters, R. (1991) <sup>32</sup>P-Postlabeling analysis and micronuclei induction in primary chinese hamster lung cells exposed to tobacco particulate matter. *Carcinogenesis* **12**, 1507-1514.
- (31) Gorelick, N. J., and Wogan, G. N. (1989) Fluoranthene-DNA adducts: identification by an HPLC-<sup>32</sup>P-postlabeling method. *Carcinogenesis* **10**, 1567-1577.
- (32) Jerina, D. M., Yagi, H., Thakker, D. R., Sayer, T. M., van Bladern, P. J., Lehr, R. E., Whalen, D. L., Levin, W., Chang, R. L., Wood, A. W., and Conney, A. N. (1984) Identification of the ultimate carcinogenic metabolites of the polycyclic aromatic hydrocarbons: bay-region (*R,S*)-diol-(*S,R*)-epoxides. In *Foreign Compound Metabolism* (Caldwell, J., and Paulson, G. D., Eds.) pp 257-266, Taylor and Francis, Ltd., London.
- (33) Levin, W., Wood, A. W., Chang, R. L., Ittah, Y., Croisy-Delcey, M., Yagi, H., Jerina, D. M., and Conney, A. H. (1980) Exceptionally high tumor-initiating activity of benzo[*c*]phenanthrene bay-region diol epoxides on mouse skin. *Cancer Res.* **40**, 3910-3914.
- (34) Baer-Dubowska, W., Frayssinet, C. H., and Alexandrov, K. (1981) Formation of covalent deoxyribonucleic acid benzo[*a*]pyrene-4,5-epoxide adduct in mouse and rat skin. *Cancer Lett.* **14**, 125-129.
- (35) Bigger, C. A. H., Tomaszewski, J. E., and Dipple, A. (1978) Differences between products of binding of 7,12-dimethylbenz[*a*]anthracene to DNA in mouse skin and in a rat liver microsomal system. *Biochem. Biophys. Res. Commun.* **80**, 229-235.
- (36) Fu, P. P., Harvey, R. G., and Beland, F. A. (1978) Molecular orbital theoretical prediction of isomeric products formed from reactions of arene oxides and related metabolites of polycyclic aromatic hydrocarbons. *Tetrahedron* **34**, 857-866.
- (37) Ashurst, S. W., and Cohen, G. M. (1982) The formation of benzo[*a*]pyrene deoxyribonucleoside adducts in vivo and in vitro. *Carcinogenesis* **3**, 267-273.
- (38) Boroujerdi, M., Kung, H., Wilson, A. G. E., Anderson, M. W. (1981) Metabolism and DNA binding of benzo[*a*]pyrene in vivo in the rat. *Cancer Res.* **41**, 951-957.
- (39) Baird, W. M., and Brookes, P. (1973) Isolation of the hydrocarbon-deoxyribonucleoside products from the DNA of mouse embryo cells treated in culture with 7-methylbenz[*a*]anthracene-<sup>3</sup>H. *Cancer Res.* **33**, 2378-2385.
- (40) Nair, R. V., Baer-Dubowska, W., Harvey, R. G., and DiGiovanni, J. (1990) Characterization of covalent DNA adducts from dibenz[*a,j*]anthracene [DB(*a,j*)A] and its 7-methyl analog [7Me-DB(*a,j*)A] in mouse epidermis. *Proc. Am. Assoc. Cancer Res.* **31**, A556.
- (41) Lecoq, S., Pfau, W., Grover, P. L., and Phillips, D. H. (1992) HPLC separation of <sup>32</sup>P-postlabelled DNA adducts formed dibenz[*a,h*]anthracene in skin. *Chem. Biol. Interact.* **85**, 173-185.
- (42) Weyand, E. H., Cai, Z. W., Wu, Y., Rice, J. E., He, Z. M., and La Voie, E. J. (1993) Detection of the major DNA adducts of benzo[*b*]fluoranthene in mouse skin: role of phenolic dihydrodiols. *Chem. Res. Toxicol.* **6**, 568-577.
- (43) Hodgson, R. M., Weston, A., and Grover, P. L. (1983) Metabolic activation of chrysene in mouse skin: evidence for the involvement of triol-epoxide. *Carcinogenesis* **4**, 1639-1643.
- (44) Pfau, W., Lecoq, S., Hughes, N. C., Seidel, A., Platt, K. L., Grover, P. L., and Phillips, D. H. (1993) Separation of <sup>32</sup>P-labelled nucleoside 3',5'-bisphosphate adducts by HPLC. In *Postlabelling methods for detection of DNA adducts* (Phillips, D. H., Castegnaro, M., and Bartsch, H., Eds.) pp 233-242, IARC, Lyon.
- (45) Caramichael, P. L., Platt, K. L., Ni She, M., Lecoq, S., Oesch, F., Phillips, D. H., and Grover, P. L. (1993) Evidence for the involvement of bis-diol epoxide in the metabolic activation of dibenz[*a,h*]anthracene to DNA-binding species in mouse skin. *Cancer Res.* **53**, 944-948.
- (46) Nair, R. V., Nettikumara, A. N., Cortez, C., Harvey, R. G., and DiGiovanni, J. (1992) Comparative metabolism of dibenz[*a,j*]anthracene and 7-methyldibenz[*a,j*]anthracene in primary cultures of mouse keratinocytes. *Chem. Res. Toxicol.* **5**, 534-540.
- (47) Lecoq, S., Chalvet, O., Strapelias, H., Grover, P. L., Phillips, D. H., and Duquesne, M. (1991) Microsomal metabolism of dibenz[*a,c*]anthracene, dibenz[*a,h*]anthracene and dibenz[*a,j*]anthracene to bisdihydrodiols and polyhydroxylated products. *Chem. Biol. Interact.* **80**, 261-279.
- (48) Mlcoch, J., Fuchs, J., Oesch, F., and Platt, K. L. (1993) Characterization of DNA adducts at the bay region of dibenz[*a,h*]anthracene formed in vitro. *Carcinogenesis* **14**, 469-473.
- (49) Segerback, D., and Vodicka, P. (1993) Recoveries of DNA adducts of polycyclic aromatic hydrocarbons in the <sup>32</sup>P-postlabelling assay. *Carcinogenesis* **14**, 2463-2469.
- (50) Hemminki, K., Szyfter, K., Vodicka, P., Koivisto, P., Mustonen, R. A., and Reunanen, A. (1991) Quantitative aspects of <sup>32</sup>P-postlabeling. In *New Horizons in Biological Dosimetry* (Gledhill, B. L., and Mauro, F., Eds.) pp 219-228, Wiley-Liss, New York, NY.

TX940123V